Guidelines for Arranging 2D Nanosheets into Neatly Tiled Monolayer Films by Spin-Coating Process

Nobuyuki Sakai and Takayoshi Sasaki*

International Center for Materials Nanoarchitectonics (WPI-MANA), National Institute for Materials Science (NIMS), 1-1 Namiki, Tsukuba, Ibaraki 305-0044, Japan

Keywords. 2D materials, neat monolayer tiling, spin-coating, air/liquid interface, hierarchical film

Abstract. Neat (dense and non-overlapped) monolayer tiling of 2D nanosheets on a substrate surface is very important because we can conduct artificial lattice-engineering by repeating the tiling process in a designed sequence to tailor various hierarchical nanostructures, leading to a range of sophisticated functions. It is recently reported that a facile spin-coating technique realizes the neat monolayer tiling of various 2D nanosheets. Establishing universal guidelines to neatly tile 2D nanosheets on substrates of various materials and size/shape is of essential importance to fully apply this technique, but the mechanism how the nanosheets are tiled has not been clarified yet. In the present study, we have systematically examined the nanosheet deposition process at various rotation speeds by microscopic observations and found that the neat monolayer tiling of nanosheets is attained on the solvent surface during the spin-coating,

and then the monolayer film is deposited onto the substrate surface from its center toward the edges upon evaporation of the solvent. Furthermore, we have clarified how the rotation speed and the nanosheet concentration govern the deposition behaviors in terms of neat tiling, overlap, or non-coverage in a such process. On the basis of the guidelines, we can predict the optimum spin-coating conditions for attaining the neat monolayer tiling of various nanosheets over an entire surface of the substrate.

Introduction

A variety of molecularly thin 2D nanosheets, which are obtained via exfoliation of their mother layered compound into single layers, have been extensively studied in the past decades, pursuing their various fascinating properties.[1–7] To design a nanodevice by fully utilizing their functions, it is important to arrange the 2D nanosheets on a substrate into precisely controlled mono- and multilayer structures. Since many of the 2D nanosheets including metal oxide nanosheets are obtained, being monodispersed in liquids, the nanosheets can be deposited on a substrate through various solution processes such as electrostatic self-assembly and Langmuir–Blodgett (LB) deposition.[8–11]

The electrostatic self-assembly method utilizes the electrostatic attraction forces working between the nanosheets and oppositely charged polymers. For example, negatively charged titania nanosheets are adsorbed on the substrate surface precoated with cationic polymers such as polyethylenimine.[9] When the substrate surface is fully covered with the nanosheets, the nanosheets dispersed in their suspension no longer adsorb on the substrate surface due to electrostatic repulsion, forming a monolayer film of the nanosheets. However, such films are not ideally monolayer, having substantial overlaps and gaps. In contrast, the LB deposition is involved by transfer of a monolayer film of the nanosheets formed on a solvent surface onto a substrate surface.[10,11] The nanosheets tend to adsorb on a solvent surface via electrostatic

interaction with amphiphilic tetrabutylammonium (TBA^+) ions. The nanosheets floating sparsely on the solvent surface are gathered and laterally packed by the surface compression with barriers under an optimized surface pressure, and the nanosheet film is transferred onto a substrate surface when the substrate immersed in the liquid is lifted to air. Although these processes can be repeated to design various hierarchical nanostructures of 2D nanosheets, leading to advanced functionalities, it is not suitable for practical industrialization because of complicated procedure and long process time.

The fabrication of thin films of 2D nanosheets has also been achieved by the spin-coating method. For example, titanium oxide and calcium niobium oxide nanosheets have been spin-coated into lamellar films with a thickness ranging from sub-micrometers to micrometers, which can be controlled by the concentration of the precursor suspension.[12,13] Apart from such conventional films, it is of greater importance to control the thickness at nanometer-scale precision or the step of nanosheet thickness, including the formation of monolayers of 2D nanosheets. Actually, neat monolayer tiling of 2D nanosheets was demonstrated by spin-coating a colloidal suspension of nanosheets under suitable conditions.[14–17] The procedure is quite simple and can be completed in a few minutes, which is highly promising for practical applications. Furthermore, repetition of the monolayer deposition in a designed sequence can construct various hierarchical nanostructures such as multilayers and superlattice- and mosaic-like heterostructured films composed of titanium oxide and calcium niobium oxide nanosheets.[17]

Understanding on how 2D nanosheets are neatly tiled in the spin-coating process is of essential importance to fully apply this technique. In previous studies, it was considered that the neat monolayer tiling of 2D nanosheets with the thickness of 1–2 nm is driven by centrifugal forces upon spin-coating,[16] as follows. The nanosheets dispersed in a suspension on a substrate surface are transported toward the substrate edges by the centrifugal forces upon

high-speed rotation of the substrate (1000–4500 rpm), and then the nanosheets are packed side-by-side from the edge of the substrate surface toward the center to form a monolayer film of neatly tiled nanosheets within a few minutes. This mechanism is based on the observation that gaps between the nanosheets are small in the area near the edges, and when the amount of nanosheets is insufficient, uncoated regions are left in the central region of the substrate surface. However, the above mechanism for the tiling of nanosheets may not be plausible because of the following reasons. The centrifugal forces (17–340*g* even at the edge of the substrate) applied to the nanosheets during the spin-coating are too small to transport the nanosheets toward the edges of the substrate (30 mmφ in diameter) within a few minutes. In fact, the nanosheets do not settle even when the suspension in a tube of similar size is centrifuged at 2300*g* for 10 min (Figure S1, Supporting Information). In addition, the above mechanism in which the nanosheet tiling ends at the center of the substrate surface is inconsistent with the fact that the drying begins from the center of the substrate surface during the spin-coating.

Since the nanosheets have extremely high 2D anisotropy with the molecularly thin thickness of 1–2 nm and the lateral dimension over several micrometers, it is of significant importance to gain the understanding for how the neat monolayer tiling of nanosheets is attained in the spin-coating process. In the present study, we have systematically examined how the nanosheets are assembled on a substrate surface depending on key parameters of the spin-coating such as the rotation speed, the concentration of nanosheet suspension, and the size of the substrate surface. On the basis of these results, the mechanism for the neat monolayer tiling is discussed. We have established the general guideline to predict deposition parameters, with which a high-quality monolayer film of well-packed nanosheets is obtained.

Results and Discussion

We carried out the spin-coating of $Ti_{0.87}O_2^{0.52-}$ nanosheets suspended in dimethyl sulfoxide (DMSO) with the concentration of 0.1 wt % on a flat surface (15 mm × 15 mm) of the indium tin oxide (ITO) substrate at various rotation speeds, and collected scanning electron microscopy (SEM) images across the entire surface of the substrate. For the sample spin-coated at 3200 rpm, the bright and dark areas were observed at the center and periphery of the substrate, respectively, and a boundary between them was distinctly recognized (Figure 1A). Since the nanosheets are discerned as darker objects than the ITO substrate as shown in the magnified SEM images, the bright area corresponds to an uncovered area that the nanosheets are sparsely adsorbed and most of the bare substrate surface is exposed (Figure 1B, C). The shape of the uncovered region was roughly square, reflecting the shape of the substrate surface. In contrast, the dark area corresponds to a covered area that the nanosheets are laterally assembled in a single layer (Figure 1D, E). The width of the uncovered area was ~9 mm, and the width of the two covered areas surrounding the uncovered area was ~3 mm each. When the sample was prepared at the rotation speed of 1800 rpm, on the other hand, the entire substrate surface looked uniform in the SEM image and no bright region was observed (Figure 1F). As revealed by the magnified SEM images, the whole surface of the substrate was covered with a monolayer film of neatly tiled nanosheets, leaving small gaps between the nanosheets (Figure 1G–J). The gap in the center region was relatively larger than that at the periphery of the substrate, and the overlaps of nanosheets into bilayers were noticeable near the edges. The neatly tiled nanosheets on an Si wafer were also observed by atomic force microscopy (AFM), as shown in Figure 2A. The thickness of the nanosheets was ~1.2 nm (Figure 2B), confirming the monolayer deposition of the nanosheets.[11] Based on the height histogram of the AFM image (Figure 2C), the coverage and the overlapped region were estimated to be 96.1% and 7.5%, respectively, indicating that the nanosheets were well-packed into a high-quality monolayer film. Similarly, we examined the spin-coated films prepared at various rotation speeds (Figure

S2, Supporting Information). When the rotation speed was 2250 rpm or higher, an uncovered region was observed in the center of the substrate surface, and its width expanded as the rotation speed increased (Figure 3A). For the samples spin-coated at 2000 rpm or lower, on the other hand, the substrates were completely covered with a film of neatly tiled nanosheets. However, overlaps of the nanosheets were also observed even at the central region of the substrate surface when spin-coated at 1690 rpm and below, and the density of overlaps increased as the rotation speed decreased (Figure 4). On the basis of the above results, it is considered that the optimum rotation speed (ω_{opt}) ranges around 1800–2000 rpm for the neat monolayer tiling of nanosheets over the entire substrate surface under the present conditions.

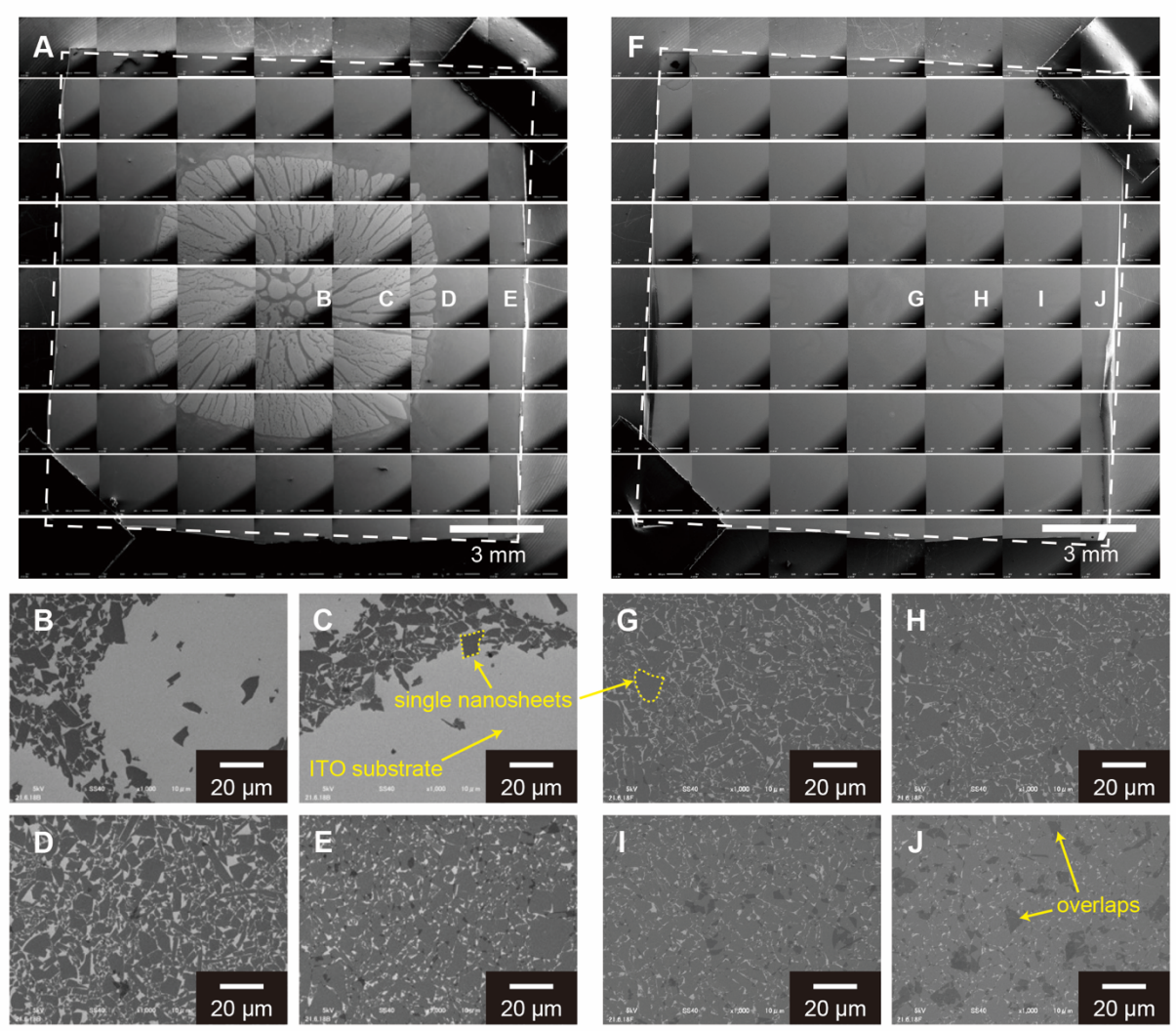

Figure 1. (A, F) Assembly of SEM images of $Ti_{0.87}O_2^{0.52-}$ nanosheets on a flat ITO substrate (15 mm × 15 mm) spin-coated at (A–E) 3200 and (F–J) 1800 rpm. The concentration of $Ti_{0.87}O_2^{0.52-}$ nanosheet suspension used for the spin-coating was 0.1 wt %. Magnified images were collected at (B, G) 1 mm, (C, H) 3 mm, (D, I) 5 mm, (E, J) 7 mm apart from the center of the substrate surface, the locations of which are indicated in the images (A, F). The square with a dashed line in the images (A, F) indicates the position of the substrate edge.

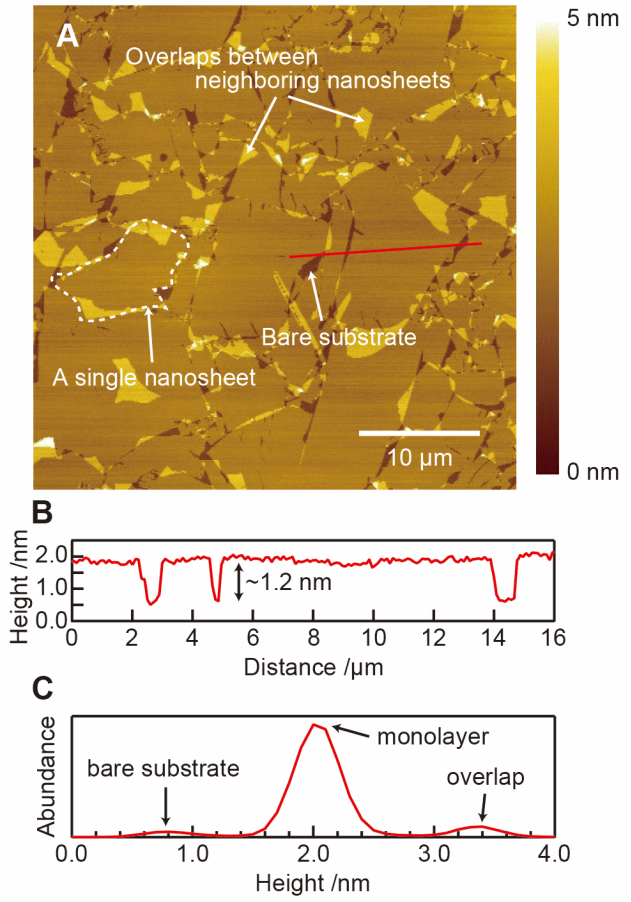

Figure 2. (A) AFM image of the $Ti_{0.87}O_2^{0.52-}$ nanosheets on an Si wafer (15 mm × 15 mm) spin-coated with $Ti_{0.87}O_2^{0.52-}$ nanosheet suspension (0.1 wt %) at 2000 rpm. (B) Cross sectional profile along with a red line shown in the AFM image. (C) Height histogram of the AFM image.

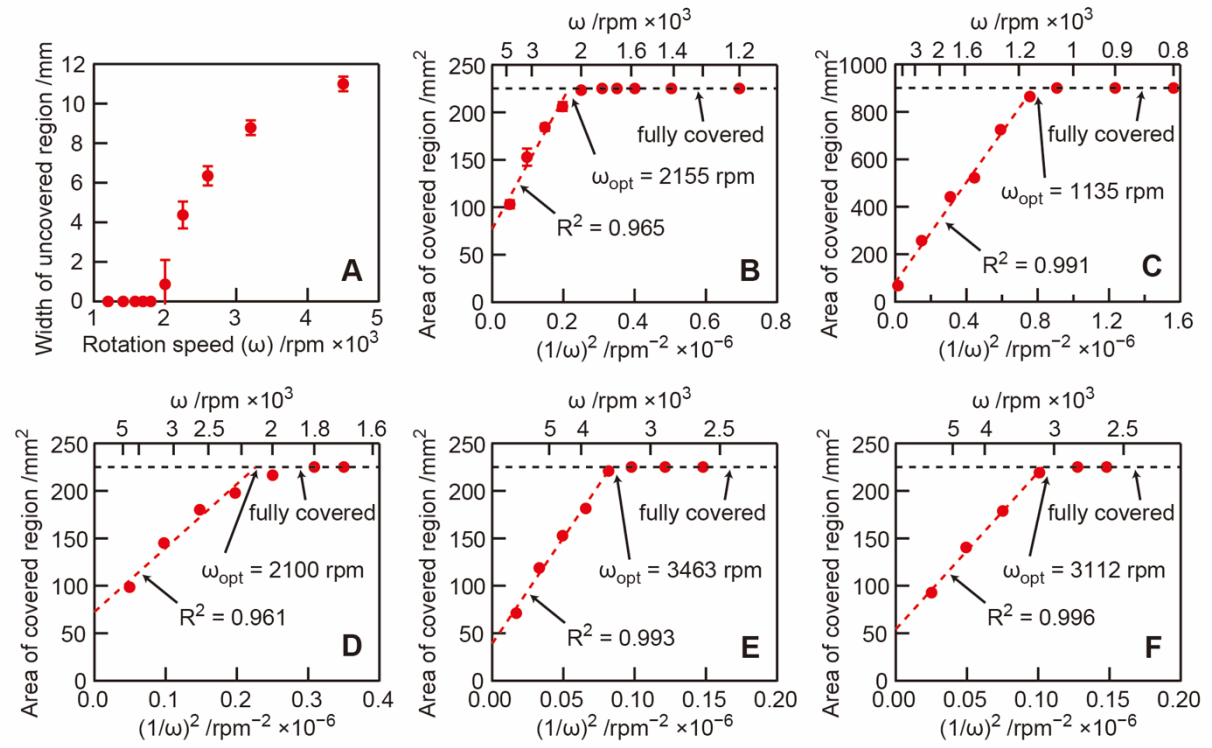

Figure 3. (A) Width of the uncovered region at the center of the flat ITO substrate (15 mm × 15 mm) plotted against the rotation speed (ω) upon spin-coating with $Ti_{0.87}O_2^{0.52-}$ nanosheet suspension (0.1 wt %). (B–F) Area of the covered region plotted as a function of $1/\omega^2$: (B) a flat ITO substrate (15 mm × 15 mm) with $Ti_{0.87}O_2^{0.52-}$ nanosheet suspension (0.1 wt %); (C) a flat ITO substrate (30 mm × 30 mm) with $Ti_{0.87}O_2^{0.52-}$ nanosheet suspension (0.1 wt %); bumpy ITO substrates (15 mm × 15 mm) with (D) $Ti_{0.87}O_2^{0.52-}$ nanosheet suspension (0.1 wt %), (E) $Ti_{0.87}O_2^{0.52-}$ nanosheet suspension (0.2 wt %), (F) $Ca_2Nb_3O_{10}^-$ nanosheet suspension (0.52 wt %).

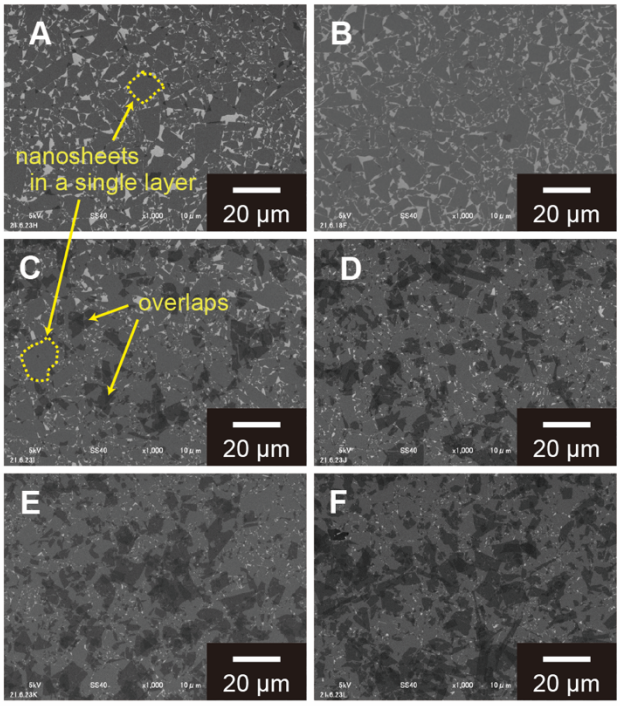

Figure 4. SEM images of $Ti_{0.87}O_2^{0.52-}$ nanosheet films at the center of the flat ITO substrate (15 mm × 15 mm) spin-coated at (A) 2000, (B) 1800, (C) 1690, (D) 1580, (E) 1410, (F) 1200 rpm. The concentration of $Ti_{0.87}O_2^{0.52-}$ nanosheet suspension used for the spin-coating is 0.1 wt %.

In order to discuss the mechanism for the neat monolayer tiling of nanosheets, we explored how the rotation speed affects the behavior of nanosheet suspension on a substrate during the spin-coating. Although most of the suspension loaded on a substrate surface is blown out of the substrate immediately after starting the high-speed rotation, a small portion of the suspension is remained to cover the substrate surface due to surface tension working at the solid/liquid interface. At the rotation speed (ω), the centrifugal force (F_c) applied to the suspension having the volume (h × the square of unit length (L)) and density (ρ) can be formulated as $F_c = L^2h\rho \times r\omega^2$ at the edge of the substrate surface, where h is the thickness of the suspension and r is the distance from the center of the substrate surface. Since the centrifugal force applied to the residual suspension is balanced with the surface tension and the

strength of the surface tension is independent of the parameters, h and ω, as far as the interface exists, a relationship of $h \propto 1/\omega^2$ can be obtained. The area (A) that can be covered with the nanosheets in a single layer is proportional to the amount of the nanosheets dispersed in the suspension, i.e., the thickness of the suspension ($A \propto h$), and hence a relationship of $A \propto 1/\omega^2$ is obtained.

Then, the area of the covered region was estimated from the SEM images and plotted against $1/\omega^2$ (Figure 3B). As expected from the above discussion, a linear relationship was obtained between A and $1/\omega^2$ ($R^2 = 0.965$) in the rotation speed range of 2200 rpm and above. The intersection of the regression line with A = 225 mm^2 (the area of the substrate surface) gives ω_{opt} = 2155 rpm, which is considered to yield that the coverable area by the nanosheets existed in the suspension is equal to the area of the substrate surface. To confirm this, we estimate the amount of nanosheets loaded on the substrate. The area that can be covered with the $Ti_{0.87}O_2^{0.52-}$ nanosheets loaded on a substrate (0.1 wt % in DMSO, 60 μL) is estimated to be ~3 × 10^4 mm^2, based on the mass of the $Ti_{0.87}O_2^{0.52-}$ nanosheet per area (2.2 × 10^{-3} g m^{-2})[17] and the density of DMSO (1.10 g cm^{-3}). The coverable area by the nanosheets is ~133 times larger than the area of the substrate surface (15 × 15 mm^2). Since the average thickness of the suspension on the substrate prior to the high-speed rotation is estimated to be ~267 μm by considering the loaded volume of the suspension and the area of the substrate surface, it is considered that the nanosheets are dispersed at an average face-to-face interval of ~2.0 μm in the suspension. Upon starting the high-speed rotation, the concentration of the nanosheet suspension on the substrate does not change, although the amount of the suspension decreases. Since the thickness of the suspension immediately after starting the high-speed rotation (1000 rpm) is reported as ~4.5 μm when the substrate size is 30 mmφ,[16] the thickness of the suspension under the present conditions (the substrate size is 15 mm × 15 mm and the rotation speed is 2155 rpm) is estimated to be ~2.0 μm by taking the difference in centrifugal forces at

the substrate edge into account ($h \propto 1/r\omega^2$). Since the average face-to-face interval of the nanosheets is ~2.0 μm in the suspension, it was confirmed that the coverable area with the nanosheets existed in the suspension is equal to the area of the substrate surface, which is sufficient for forming a monolayer film of neatly tiled nanosheets across the entire substrate surface. Conversely, the amount of the nanosheets is insufficient when the rotation speed is larger than 2155 rpm, leaving a part of the substrate surface uncovered. The relationship of $A \propto 1/\omega^2$ was also observed when we employed different sizes of the flat ITO substrate, different substrates including bumpy ITO substrates, different concentrations of $Ti_{0.87}O_2^{0.52-}$ nanosheet suspensions, and different types of oxide nanosheets including $Ca_2Nb_3O_{10}^-$, although ω_{opt} depended on various parameters such as the size of substrates, the concentration of nanosheet suspensions, and the type of nanosheets (Figure 3C–F). It is noteworthy that the optimum rotation speed was almost the same for the bumpy ITO substrate (2100 rpm, Figure 3D) and the flat ITO substrate (2155 rpm, Figure 3B), despite of the different surface morphology.

We attempted ex-situ observation on how the monolayer film of nanosheets is formed on a substrate surface on the basis of the different surface coverage of nanosheets depending on the rotation speed (Figure 3C). The surface of a flat ITO substrate (30 mm × 30 mm) was fully covered with a monolayer film of neatly tiled nanosheets when spin-coated at 1050 rpm for 300 s until the substrate surface was completely dried (Figure S3A–E, Supporting Information), whereas most of the substrate surface was remained uncovered except for the covered region within ~1 mm from the edges when spin-coated at 8000 rpm (Figure S3F–J, Supporting Information). Hence, if the rotation speed is switched from 1050 rpm to 8000 rpm during drying, it is expected that a state on a half way to the fully covered is captured. We performed the spin-coating of $Ti_{0.87}O_2^{0.52-}$ nanosheets on a flat ITO substrate (30 mm × 30 mm) at 1050 rpm for 210 s and switched to 8000 rpm in the mid-course of drying, and held it for 120 s until the surface was dried. As observed by SEM (Figure 5A), monolayer films of neatly tiled

nanosheets were observed in the regions within 9–10 mm from the center of the substrate (Figure 5B) and within ~1 mm from the edges (Figure 5D), and the nanosheets were sparsely adsorbed between these two regions (Figure 5C). It is considered that the monolayer film in the central region was formed during the rotation at 1050 rpm, since the center region of the substrate surface was uncovered when spin-coated at 8000 rpm from the beginning. In contrast, the neat monolayer tiling of nanosheets near the edges was attained during the rotation at 8000 rpm, as observed when spin-coated at 8000 rpm from the beginning. The region in between the above two domains of the monolayer film was remained uncovered as a result of the switching of the rotation speed from 1050 rpm to 8000 rpm in the mid-course of the drying of the substrate surface. Hence, it was confirmed that the monolayer film of neatly tiled nanosheets starts to form from the center of the substrate surface and spreads toward the edges.

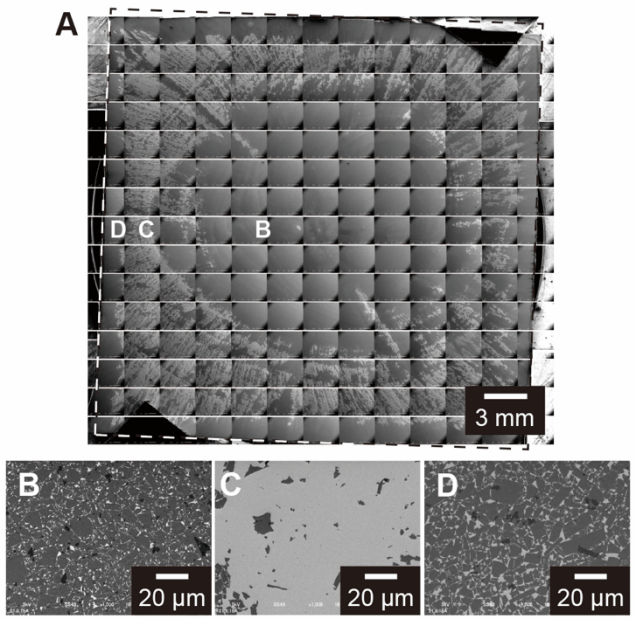

Figure 5. (A) Assembly of SEM images of $Ti_{0.87}O_2^{0.52-}$ nanosheets spin-coated on a flat ITO substrate (30 mm × 30 mm). The spin-coating of $Ti_{0.87}O_2^{0.52-}$ nanosheets (0.1 wt %) was performed at the rotation speed of 1050 rpm for 210 s followed by the rotation at 8000 rpm for 120 s. The square with a dashed line indicates the position of the substrate edge. Magnified

images were collected at (B) 4 mm, (C) 12 mm, (D) 14 mm apart from the center of the substrate surface, the locations of which are indicated in the image (A).

Next, we discuss the mechanism for the neat monolayer tiling of nanosheets. Since the formation of the monolayer film begins from the center of the substrate surface and spread toward the edges, one might think that the tiling of nanosheets is based on the convective self-assembly, which is similar to the formation process of a laterally assembled monolayer film of spherical nanoparticles, also called 2D colloidal crystals.[18–21] In the convective self-assembly process, when the tops of the particles with a diameter of several hundred nanometers protrude from the suspension upon evaporation of the solvent during the spin-coating, capillary attraction forces are generated due to the menisci formed between the particles, forming the core of the 2D colloidal crystal at the center of the substrate surface. As the surrounding solvent evaporates, the particles gather to grow the colloidal crystal toward the edges of the substrate, forming the 2D colloidal crystal over the entire surface of the substrate.[22–24] In the case of the nanosheets, however, bringing the attraction forces into action as the case for convective self-assembly will be extremely unfavorable because the meniscus shape will not be expected for their gap considering their very high 2D geometry. Furthermore, the thickness of the suspension should be smaller than the nanosheet thickness of ~1.2 nm, which corresponds to 4 molecules or less of DMSO. It is unlikely that such a thin layer of DMSO molecules behaves as a rheological liquid to show viscoelasticity, and the DMSO molecules will evaporate completely before the nanosheets are tiled. In addition, it is reported that the flatness of substrate surfaces is important for the formation of highly ordered 2D colloidal crystals in a monolayer.[25] Conversely, the monolayer film of neatly tiled nanosheets was obtained not only on the flat surfaces but also on the bumpy surfaces (Figure 3), the roughness of which is much larger than the nanosheet thickness (Figure S4, Supporting Information). Hence, it is

considered that the nanosheet monolayer tiling is not resulted from the event on the substrate surface.

We propose another mechanism, i.e., the monolayer film of neatly tiled nanosheets is formed on a solvent surface and transferred onto a substrate surface during the spin-coating process (Figure 6), which is similar to the case of the LB method.[10,11] In the LB method, a monolayer film of laterally packed nanosheets is formed at the air/liquid interface under an optimized surface pressure, and the nanosheet film is transferred onto a substrate surface when the substrate immersed in the liquid is lifted to air. We speculate that essentially the same event occurs in the film formation by the spin-coating method. First, we discuss how the neat monolayer tiling of nanosheets is attained on the solvent surface during the spin-coating process. In the aqueous suspension, the nanosheet surface is covered with TBA^+ ions, which work as amphiphilic agents, and thus the nanosheets tend to be trapped at the air/liquid interface because the hydrophobic butyl chains of TBA^+ ions escape from aqueous solution, pointing toward the gas phase.[10,15,26–28] Such nanosheets floating sparsely on the solvent surface are gathered and laterally packed by the surface compression with barriers in the LB method. The nanosheets may be trapped at the air/liquid interface also in the DMSO during the spin-coating process. The TBA^+ ions most likely show amphiphilic property in DMSO because DMSO is miscible with water. As the suspension becomes thinner due to evaporation of the solvent during the spin-coating, the nanosheets will be trapped more easily due to increased concentration of nanosheets in the suspension as well as shortened distance to the solvent surface. As a result, the amount of the trapped nanosheets is increased to fully cover the solvent surface under the rotation speed of ω_{opt} and below (Figure 6, i to iii). In this process, it is important to point out that the overlap of the nanosheets on the solvent surface is avoided due to electrostatic repulsion between the nanosheet faces, increasing the nanosheet population at the surface and then leading to well-packed arrangement of the nanosheets. At an optimum

rotation speed, a monolayer film of neatly tiled nanosheets is formed on a solvent surface and then transferred onto a substrate surface as the substrate is dried from the center to the edges (Figure 6, iii to vi). It is noted that the tiling on the solvent surface needs to be completed before the drying of the substrate surface begins. This transfer model is consistent with the fact that the difference of surface morphology and flatness of the substrate did not affect the optimum conditions for the monolayer tiling of nanosheets as mentioned above.

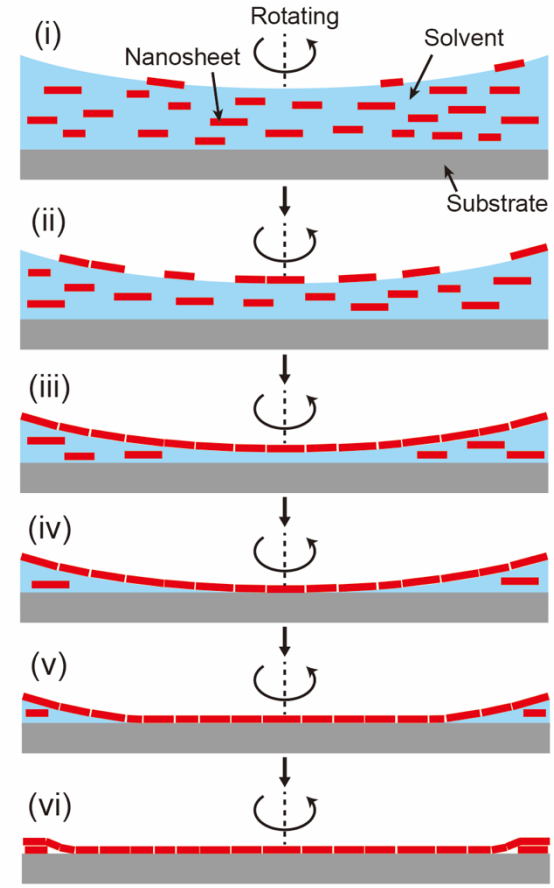

Figure 6. Schematic illustration of the formation process of a monolayer film of neatly tiled nanosheets on a substrate surface during the spin-coating. (i) Upon the rotation, a small portion of the suspension is remained to cover the substrate surface. (ii) The nanosheets are trapped at the air/liquid interface. (iii) Neat monolayer tiling of nanosheets is attained on the solvent surface. (iv) The monolayer film is deposited onto the substrate surface as the substrate is dried

from the center. (v) As the drying proceeds, the region of the monolayer film on the substrate surface expands toward the edges of the substrate. (vi) The transfer is completed to form a monolayer film of neatly tiled nanosheets on the substrate surface with some overlaps near the edges.

The model in which the nanosheet film formed on the solvent surface is deposited onto the substrate surface in the spin-coating process can explain the observed result that the gaps between the neighboring nanosheets in the center region of the monolayer film formed on the substrate surface are wider than those in the periphery of the substrate. In the beginning of the transfer, the monolayer film of neatly tiled nanosheets formed on the solvent surface is deposited onto a substrate surface keeping the relatively wide gaps. As the deposition proceeds, the density of nanosheets on the solvent surface is increased due to evaporation of the solvent, resulting in the narrower gaps in the monolayer film on the solvent surface. Hence, the gaps between the nanosheets near the edges are narrower compared to those at the center of the substrate surface.

The model can also elucidate the different adsorption behaviors of the nanosheets on the substrate surface, depending on the rotation speed. When the rotation speed is larger than ω_{opt}, the amount of nanosheets in the suspension remained upon the rotation is insufficient for the full coverage of the substrate surface, and the trapped nanosheets are sparsely present at the air/liquid interface. As the area of the solvent surface becomes smaller due to partial drying of the substrate surface, however, the density of the trapped nanosheets is increased to attain the neat monolayer tiling of the nanosheets on the remained solvent surface, and then the monolayer film is deposited onto the substrate surface. As a result, a monolayer film of neatly tiled nanosheets is formed at the periphery region of the substrate surface, remaining the center region uncovered (Figure 1A).

When the rotation speed is smaller than ω_{opt}, on the other hand, the amount of nanosheets remained after the rotation begins exceeds the threshold value to fully cover the substrate surface. Hence, in addition to the monolayer film of nanosheets formed on the solvent surface being deposited to the substrate surface, the nanosheets suspended in the solvent adsorb on the substrate upon complete evaporation of the solvent, resulting in the overlaps of the nanosheets. Actually, the density of the overlapped nanosheets was increased as the rotation speed was decreased (Figure 4). The overlap of the nanosheets occurs between an isolated nanosheet and a part of the neatly tiled nanosheets (Figure 1I, J). It is expected that the isolated nanosheets are sandwiched between the neatly tiled nanosheets and the substrate surface, because such isolated nanosheets originate from those suspended in the solvent and the film of neatly tiled nanosheets is formed on the solvent surface during the spin-coating. This is experimentally supported by the cross sectional profile of overlapped region examined by AFM. We observed several isolated $Ca_2Nb_3O_{10}^-$ nanosheets in addition to neatly tiled nanosheets (Figure 7A). The cross section was examined in the area where an isolated nanosheet was overlapped with two nanosheets of the neatly tiled nanosheets, and the height of the isolated nanosheets in the gap between the two nanosheets was lower than that of the two nanosheets (Figure 7B), indicating that the isolated nanosheet is located beneath the film of neatly tiled nanosheets. The overlaps of the nanosheets are hardly seen in the LB method,[11] because the nanosheet suspension is not completely evaporated during the LB process, which is different from the spin-coating process. Such isolated nanosheets adsorb on the substrate surface when the suspension becomes completely dried, which is consistent with the observed result that the overlapped nanosheets were more frequently found near the edges of the substrate (Figure 1G–J).

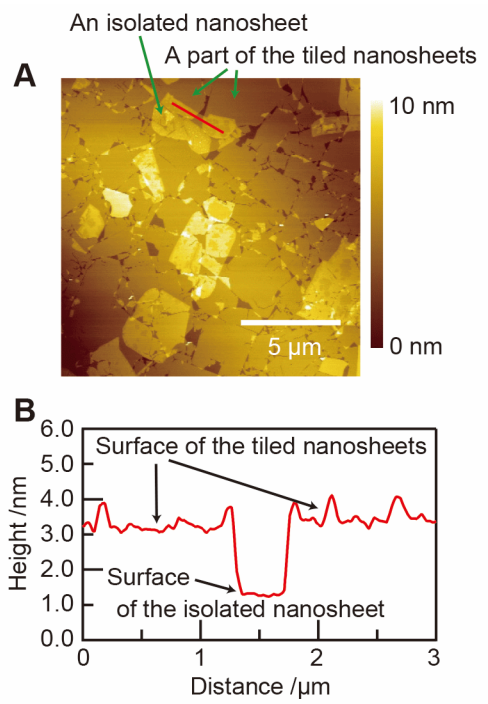

Figure 7. (A) AFM image of the $Ca_2Nb_3O_{10}^-$ nanosheets on an Si wafer spin-coated with $Ca_2Nb_3O_{10}^-$ nanosheet suspension (0.52 wt %) at 2500 rpm. (B) Cross sectional profile along with a red line shown in the AFM image.

Conclusion

We have performed the microscopic observation of the whole-area of substrate surface to systematically examine the area of a monolayer film of neatly tiled nanosheets formed at various rotation speeds (ω) in the spin-coating process, and found that the area (A) covered with the monolayer film is linearly dependent on the reciprocal of the square of the rotation speed ($A \propto 1/\omega^2$). This relationship is valuable to predict the optimum rotation speed for attaining a neat monolayer tiling of nanosheets, which is dependent on the size of substrates, the concentration of nanosheet suspensions, and the type of nanosheets. We have also clarified how the monolayer film of neatly tiled nanosheets is formed on a substrate surface via the spin-coating. The nanosheets are trapped at the air/liquid interface, and their density increases as the thickness of the suspension decreases, leading the self-assembly of the trapped nanosheets to

attain their neat monolayer tiling on the solvent surface. The monolayer film of neatly tiled nanosheets formed on the solvent surface is deposited onto a substrate surface from the center of the substrate toward the edges upon drying the substrate surface at an appropriate rotation speed. The knowledge obtained in this work would facilitate the utilization of spin-coating technique for constructing precisely organized hierarchical films based on a variety of 2D nanosheets, developing sophisticated functions.

Methods

Reagents and Materials. All chemicals were of analytical grade and used as purchased. Milli-Q filtered water was used throughout the experiments. Polished ITO (180 nm thick)-coated glass plates with flat surfaces were obtained from Kuramoto Co., Japan. Unpolished ITO (220 nm thick)-coated glass plates with bumpy surfaces and Si (100) wafers were purchased from Furuuchi Chemical Co., Japan.

Preparation of Nanosheet Suspensions. An aqueous colloidal suspension of $Ti_{0.87}O_2^{0.52-}$ nanosheets was prepared following a previously reported procedure (Figure S5, Supporting Information).[29–31] A stoichiometric mixture of TiO_2, K_2CO_3, and Li_2CO_3 powders was annealed at 1000 °C for 20 h to synthesize a lepidocrocite-type layered titanate, $K_{0.8}Ti_{1.73}Li_{0.27}O_4$, and then it was treated with 1 M HCl solution at ambient temperature for 72 h to yield a protonated phase. The obtained $H_{1.07}Ti_{1.73}O_4 \cdot H_2O$ was dispersed in a TBA hydroxide solution (TBA^+/H^+ = 1) and shaken intermittently for a period of 1 month to be exfoliated. The resulting suspension contained unilamellar nanosheets of $Ti_{0.87}O_2^{0.52-}$ with a lateral size of tens of micrometers and a thickness of ~1.2 nm. The aqueous suspension was centrifuged at 10000 rpm (9300*g*) for 30 min, and the resulting sediment was dispersed in DMSO to obtain DMSO suspensions of $Ti_{0.87}O_2^{0.52-}$ nanosheets. The mass concentration of the nanosheets in the DMSO suspension was estimated by absorbance of the suspension diluted with DMSO, molar extinction

coefficient, and density of DMSO (ρ = 1.10 g cm^{-3}). The molar extinction coefficient (ε) was determined by the combination of spectroscopic analysis and gravimetric quantification of the solid content upon heating at 1000 °C: $\varepsilon = 1.12(1) \times 10^4$ (n = 3) mol^{-1} dm^3 cm^{-1} at 270 nm for the $Ti_{0.87}O_2^{0.52-}$ nanosheets suspended in DMSO.[32]

A DMSO suspension of $Ca_2Nb_3O_{10}^-$ nanosheets was prepared in a similar way.[17] A layered perovskite powder of $KCa_2Nb_3O_{10}$ was synthesized by annealing a mixture of K_2CO_3, $CaCO_3$, and Nb_2O_5 (K:Ca:Nb = 1.1:2:3) at 1200 °C for 12 h, and then it was treated with 5 M HNO_3 solution at ambient temperature for 72 h to yield a protonated phase.[33] The obtained product of $HCa_2Nb_3O_{10}\cdot 1.5H_2O$ was dispersed in a TBA hydroxide solution (TBA^+/H^+ = 1) and shaken intermittently for a period of 1 month to be exfoliated. The resulting aqueous suspension of unilamellar $Ca_2Nb_3O_{10}^-$ nanosheets was centrifuged at 15000 rpm (21000*g*) for 30 min, and the obtained sediment was dispersed in DMSO. The concentration of the DMSO suspension of $Ca_2Nb_3O_{10}^-$ nanosheets was estimated by using $\varepsilon = 2.03(2) \times 10^4$ (n = 3) mol^{-1} dm^3 cm^{-1} at 270 nm for the $Ca_2Nb_3O_{10}^-$ nanosheets suspended in DMSO.

Spin-Coating of Nanosheets. ITO substrates (15 mm × 15 mm or 30 mm × 30 mm) were cleaned with acetone and then treated with oxygen plasma by a plasma ion bombardment (PIB-20, Vacuum Device, Japan) to turn their surface hydrophilic. The substrate was then placed onto the sample holder of a spin coater (MS-B100, Mikasa, Japan), covered with a DMSO suspension (60 μL or 180 μL) of nanosheets at a designated concentration, and spun at the designated rotation speed (ω) for 300 s. The temperature was strictly regulated at 26.5 ± 0.1 °C during the spin-coating. When the temperature was deviated by 0.3–0.6 °C, the optimum rotation speed was varied 4–8% as $1/\omega^2$, probably due to the difference in the temperature-dependent vapor pressure of the suspension.

Apparatus. SEM images were acquired at an accelerating voltage of 5 kV (JSM-6010LA, JEOL, Japan). AFM images were collected in tapping mode using a scanning probe microscopy

(E-sweep, Hitachi High-Tech Science, Japan) equipped with a cantilever (SI-DF20). A UV–vis spectrophotometer (V-670, Jasco, Japan) was used to record absorption spectra of nanosheet suspensions.

ASSOCIATED CONTENT

Supporting Information. The following file is available free of charge.

UV-vis absorption spectra and pictures of $Ti_{0.87}O_2^{0.52-}$ nanosheet suspensions before and after centrifugation. SEM images of $Ti_{0.87}O_2^{0.52-}$ nanosheets spin-coated at various rotation speeds. AFM images of bare ITO surfaces. Synthesis procedure of $Ti_{0.87}O_2^{0.52-}$ nanosheets (PDF)

AUTHOR INFORMATION

Corresponding Author

*Nobuyuki Sakai – International Center for Materials Nanoarchitectonics (WPI-MANA), National Institute for Materials Science (NIMS), 1-1 Namiki, Tsukuba, Ibaraki 305-0044, Japan; ORCID: 0000-0002-9395-6751; E-mail: sakai.nobuyuki@nims.go.jp

Author Contributions

N.S. conceived the main idea, designed the experiments, and wrote the original manuscript. N.S. and T.S. discussed the results and revised the manuscript.

Notes

The authors declare no competing financial interests.

ACKNOWLEDGMENT

This work was partly supported by the World Premier International Research Center Initiative on Materials Nanoarchitectonics (WPI-MANA), MEXT, Japan, and CREST of the Japan Science and Technology Agency (JST) (grant no. JPMJCR17N1), Japan.

REFERENCES

(1) Geim, A. K.; Novoselov, K. S. The Rise of Graphene. *Nat. Mater.* **2007**, 6, 183–191.

(2) Novoselov, K. S.; Mishchenko, A.; Carvalho, A.; Neto, A. H. C. 2D Materials and van der Waals Heterostructures. *Science* **2016**, 353, aac9439.

(3) Chhowalla, M.; Shin, H. S.; Eda, G.; Li, L.-J.; Loh, K. P.; Zhang, H. The Chemistry of Two-Dimensional Layered Transition Metal Dichalcogenide Nanosheets. *Nat. Chem.* **2013**, 5, 263–275.

(4) Tan, C.; Cao, X.; Wu, X.-J.; He, Q.; Yang, J.; Zhang, X.; Chen, J.; Zhao, W.; Han, S.; Nam, G.-H.; Sindoro, M.; Zhang, H. Recent Advances in Ultrathin Two-Dimensional Nanomaterials. *Chem. Rev.* **2017**, 117, 6225–6331.

(5) Osada, M.; Sasaki, T. Exfoliated Oxide Nanosheets: New Solution to Nanoelectronics. *J. Mater. Chem.* **2009**, 19, 2503–2511.

(6) Ma, R.; Sasaki, T. Two-Dimensional Oxide and Hydroxide Nanosheets: Controllable High-Quality Exfoliation, Molecular Assembly, and Exploration of Functionality. *Acc. Chem. Res.* **2015**, 48, 136–143.

(7) Uppuluri, R.; Gupta, A. S.; Rosas, A. S.; Mallouk, T. E. Soft Chemistry of Ion-Exchangeable Layered Metal Oxides. *Chem. Soc. Rev.* **2018**, 47, 2401–2430.

(8) Keller, S. W.; Kim, H.-N.; Mallouk, T. E. Layer-by-Layer Assembly of Intercalation Compounds and Heterostructures on Surfaces: Toward Molecular "Beaker" Epitaxy. *J. Am. Chem. Soc.* **1994**, 116, 8817–8818.

(9) Sasaki, T.; Ebina, Y.; Tanaka, T.; Harada, M.; Watanabe, M.; Decher, G. Layer-by-Layer Assembly of Titania Nanosheet/Polycation Composite Films. *Chem. Mater.* **2001**, 13, 4661–4667.

(10) Muramatsu, M.; Akatsuka, K.; Ebina, Y.; Wang, K.; Sasaki, T.; Ishida, T.; Miyake, K.; Haga, M. Fabrication of Densely Packed Titania Nanosheet Films on Solid Surface by Use of Langmuir–Blodgett Deposition Method without Amphiphilic Additives. *Langmuir* **2005**, 21, 6590–6595.

(11) Akatsuka, K.; Haga, M.; Ebina, Y.; Osada, M.; Fukuda, K.; Sasaki, T. Construction of Highly Ordered Lamellar Nanostructures through Langmuir–Blodgett Deposition of Molecularly Thin Titania Nanosheets Tens of Micrometers Wide and Their Excellent Dielectric Properties. *ACS Nano* **2009**, 3, 1097–1106.

(12) Abe, R.; Shinohara, K.; Tanaka, A.; Hara, M.; Kondo, J. N.; Domen, K. Preparation of Thin Films of a Layered Titanate by the Exfoliation of $Cs_xTi_{(2-x/4)}\square_{x/4}O_4$. *Chem. Mater.* **1998**, 10, 329–333.

(13) Ganter, P.; Lotsch, B. V. Photocatalytic Nanosheet Lithography: Photolithography based on Organically Modified Photoactive 2D Nanosheets. *Angew. Chem. Int. Ed.* **2017**, 56, 8389–8392.

(14) Yamaguchi, H.; Eda, G.; Mattevi, C.; Kim, H.; Chhowalla, M. Highly Uniform 300 mm Wafer-Scale Deposition of Single and Multilayered Chemically Derived Graphene Thin Films. *ACS Nano* **2010**, 4, 524–528.

(15) Kim, J. W.; Kang, D.; Kim, T. H.; Lee, S. G.; Byun, N.; Lee, D. W.; Seo, B. H.; Ruoff, R. S.; Shin, H. S. Mosaic-like Monolayer of Graphene Oxide Sheets Decorated with Tetrabutylammonium Ions. *ACS Nano* **2013**, 7, 8082–8088.

(16) Matsuba, K.; Wang, C.; Saruwatari, K.; Uesusuki, Y.; Akatsuka, K.; Osada, M.; Ebina, Y.; Ma, R.; Sasaki, T. Neat Monolayer Tiling of Molecularly Thin Two-Dimensional Materials in 1 min. *Sci. Adv.* **2017**, 3, e1700414.

(17) Yano, H.; Sakai, N.; Ebina, Y.; Ma, R.; Osada, M.; Fujimoto, K.; Sasaki, T. Construction of Multilayer Films and Superlattice- and Mosaic-like Heterostructures of 2D Metal Oxide Nanosheets via a Facile Spin-coating Process. *ACS Appl. Mater. Interfaces* **2021**, 13, 43258–43265.

(18) Mihi, A.; Ocaña, M.; Míguez, H. Oriented Colloidal-Crystal Thin Films by Spin-Coating Microspheres Dispersed in Volatile Media. *Adv. Mater.* **2006**, 18, 2244–2249.

(19) Ogi, T.; Modesto-Lopez, L. B.; Iskandar, F.; Okuyama, K. Fabrication of a Large Area Monolayer of Silica Particles on a Sapphire Substrate by a Spin Coating Method. *Colloids Surf. A Physicochem. Eng. Asp.* **2007**, 297, 71–78.

(20) Zhang, J.; Li, Y.; Zhang, X.; Yang, B. Colloidal Self-Assembly Meets Nanofabrication: From Two-Dimensional Colloidal Crystals to Nanostructure Arrays. *Adv. Mater.* **2010**, 22, 4249–4269.

(21) Vogel, N.; Retsch, M.; Fustin, C.-A.; del Campo, A.; Jonas, U. Advances in Colloidal Assembly: The Design of Structure and Hierarchy in Two and Three Dimensions. *Chem. Rev.* **2015**, 115, 6265–6311.

(22) Denkov, N. D.; Velev, O. D.; Kralchevsky, P. A.; Ivanov, I. B.; Yoshimura, H.; Nagayama, K. Mechanism of Formation of Two-Dimensional Crystals from Latex Particles on Substrates. *Langmuir* **1992**, 8, 3183–3190.

(23) Kralchevsky, P. A.; Nagayama, K. Capillary Forces between Colloidal Particles. *Langmuir* **1994**, 10, 23–36.

(24) Denkov, N. D.; Velev, O. D.; Kralchevsky, P. A.; Ivanov, I. B.; Yoshimura, H.; Nagayama, K. Two-Dimensional Crystallization. *Nature* **1993**, 361, 26.

(25) Nagayama, K. Two-Dimensional Self-Assembly of Colloids in Thin Liquid Films. *Colloids Surf. A Physicochem. Eng. Asp.* **1996**, 109, 363–374.

(26) Kim, F.; Cote, L. J.; Huang, J. Graphene Oxide: Surface Activity and Two-Dimensional Assembly. *Adv. Mater.* **2010**, 22, 1954–1958.

(27) Yuan, H.; Timmerman, M.; van de Putte, M.; Gonzalez Rodriguez, P.; Veldhuis, S.; ten Elshof, J. E. Self-Assembly of Metal Oxide Nanosheets at Liquid–Air Interfaces in Colloidal Solutions. *J. Phys. Chem. C* **2016**, 120, 25411–25417.

(28) Shi, Y.; Osada, M.; Ebina, Y.; Sasaki, T. Single Droplet Assembly for Two-Dimensional Nanosheet Tiling. *ACS Nano* **2020**, 14, 15216–15226.

(29) Sasaki, T.; Watanabe, M. Osmotic Swelling to Exfoliation. Exceptionally High Degrees of Hydration of a Layered Titanate. *J. Am. Chem. Soc.* **1998**, 120, 4682–4689.

(30) Sasaki, T.; Kooli, F.; Iida, M.; Michiue, Y.; Takenouchi, S.; Yajima, Y.; Izumi, F.; Chakoumakos, B. C.; Watanabe, M. A Mixed Alkali Metal Titanate with the Lepidocrocite-Like Layered Structure. Preparation, Crystal Structure, Protonic Form, and Acid-Base Intercalation Properties. *Chem. Mater.* **1998**, 10, 4123–4128.

(31) Maluangnont, T.; Matsuba, K.; Geng, F.; Ma, R.; Yamauchi, Y.; Sasaki, T. Osmotic Swelling of Layered Compounds as a Route to Producing High-Quality Two-Dimensional Materials. A Comparative Study of Tetramethylammonium versus Tetrabutylammonium Cation in a Lepidocrocite-Type Titanate. *Chem. Mater.* **2013**, 25, 3137–3146.

(32) Sakai, N.; Suzuki, M.; Sasaki, T. Scission of 2D Inorganic Nanosheets via Physical Adsorption on a Nonflat Surface. *Adv. Mater. Interfaces* **2022**, 9, 2102591.

(33) Ebina, Y.; Sasaki, T.; Watanabe, M. Study on Exfoliation of Layered Perovskite-Type Niobates. *Solid State Ionics* **2002**, 151, 177–182.

TOC Graphic